

Structural properties of the sesquicarbide superconductor La_2C_3 at high pressure

X. Wang,¹ I. Loa,¹ K. Syassen,^{1,*} R. K. Kremer,¹ A. Simon,¹ M. Hanfland,² and K. Ahn³

¹Max-Planck-Institut für Festkörperforschung, Heisenbergstrasse 1, D-70569 Stuttgart, Germany

²European Synchrotron Radiation Facility, BP 220, F-38043 Grenoble, France

³Department of Chemistry, Yonsei University, Wonju 220-710, South Korea

(Dated: November 19, 2018)

The effect of pressure on the structural properties of lanthanum sesquicarbide La_2C_3 ($T_c = 13$ K) has been investigated at room temperature by angle-dispersive powder x-ray diffraction in a diamond anvil cell. The compound remains in the cubic Pu_2C_3 -type structure at pressures up to at least 30 GPa. The corresponding equation of state parameters are reported and discussed in terms of phase stability of La_2C_3 . Pressure-volume data of the impurity phase LaC_2 are reported also for pressures up to 13 GPa.

PACS numbers: PACS: 61.50.Ks, 62.50.+p, 77.80.Bh

I. INTRODUCTION

Superconductivity in binary rare earth carbides has been an intensively investigated topic for many years. Outstanding in this family of compounds with respect to their superconducting transition temperatures T_c are the sesquicarbides RE_2C_3 , RE being the nonmagnetic rare earth metals Y and La. These systems recently regained attention due to the finding by Amano *et al.* and Nakane *et al.* who reported the successful synthesis of binary Y_2C_3 under high pressure conditions (~ 5 GPa). They reported transition temperatures T_c and critical fields B_{c2} of 18 K and >30 T, respectively.^{1,2}

All RE carbides of composition RE_2C_3 are isotypic; they crystallize in the cubic Pu_2C_3 structure-type³ (see Fig. 1). Electronic structure calculations, based on the Pu_2C_3 structure type, have been carried out recently for Y_2C_3 by Shein *et al.* and by Singh and Mazin.^{4,5} Singh and Mazin⁵ specifically discuss the origin and magnitude of the electron-phonon coupling in Y_2C_3 . They identify low-frequency metal atom vibrations to have the largest

coupling whereas the contribution of the high-frequency C–C stretching vibrations is found to be comparatively small.

So far, the samples of Y_2C_3 showing a T_c of 18 K have been characterized by x-ray powder diffraction only. A more detailed investigation of these phases with respect to the exact composition and the phase diagram is still pending. In this respect La_2C_3 , which shows superconductivity with T_c up to 13.2 K and which can be prepared at ambient pressure, is better understood.^{6,7,8}

We report here the equation of state and the effect of pressure on the structure of La_2C_3 . The structural properties were measured up to 30 GPa using synchrotron powder x-ray diffraction in the angle-dispersive mode. Our primary motivation was to investigate how pressure affects the structural degrees of freedom of the Pu_2C_3 -type phase; these are thought to play a key role in controlling the details of the electronic structure in the vicinity of the Fermi level. Second, the equation of state and phase stability of La_2C_3 is of interest in the context of pressure synthesis of rare earth carbides. To our knowledge, pressure-dependent studies similar to the ones presented here have not been reported so far for any of the known rare earth and actinide sesquicarbides.

II. SAMPLE CHARACTERIZATION, DIFFRACTION EXPERIMENTS

The superconducting properties of La_2C_3 depend sensitively on the carbon content. Spedding *et al.* and Gschneidner *et al.* report a homogeneity regime for $\text{La}_2\text{C}_{3-x}$ which ranges from 56.2 at.-% to 60.2 at.-% carbon with cubic lattice parameters from 8.803 Å to 8.818 Å, respectively.^{6,7} Recently, Simon and Gulden reinvestigated the phase diagram of $\text{La}_2\text{C}_{3-x}$ ($0 < x < 0.33$).⁸ They find that the boundary phases with $x = 0$ and $x = 0.33$ are homogeneous but that by sufficiently extended annealing, samples within the homogeneity range tend to phase separate into the boundary phases with $x = 0$ and $x = 0.33$. According to magnetic susceptibility measurements these boundary phases have sharp

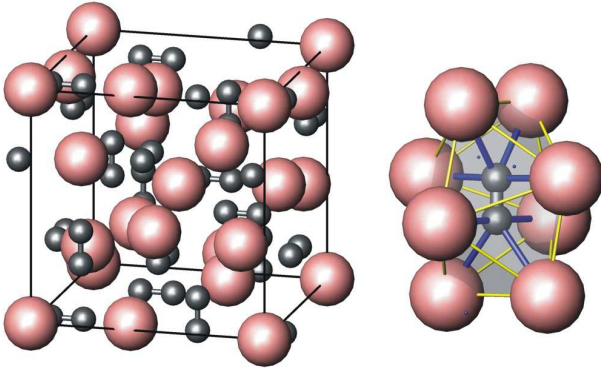


FIG. 1: (Color online) The Pu_2C_3 -type cubic crystal structure of La_2C_3 [space group (SG) $I\bar{4}3d$ (No. 220), $Z = 8$ formula units in the cubic cell]. The dicarbide anions occupy the voids in bisphenoids of the metal substructure. Note: Different from the standard crystallographic setting, the origin of the indicated unit cell is shifted into a La position.

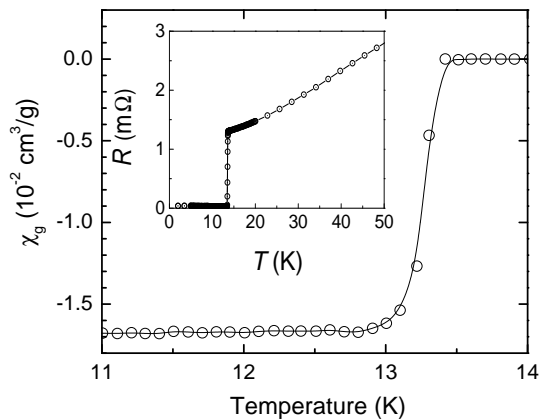


FIG. 2: Diamagnetic shielding and electrical resistance (inset) of the La_2C_3 sample used for the high-pressure x-ray diffraction experiment. The diamagnetic shielding was measured in a field of 0.7 mT after the sample had been cooled in zero field to 2 K.

superconducting transitions at 5.6 K and at 13.2 K, respectively.⁹ The latter value obtained for the stoichiometric phase La_2C_3 is appreciably increased over the early T_c of 11 K reported by Giorgi *et al.*^{10,11} The 13.2 K phase shows critical fields $B_{c2} \geq 17$ T, significantly enhanced over $B_{c2} = 12$ T found by Francavilla *et al.*¹² (see also Ref. 13).

The polycrystalline sample of La_2C_3 used in the present study was prepared by arc melting appropriate quantities of La metal (Alfa, 99.99%) and graphite chips (Deutsche Carbone, 99.99%) with a slight excess (2 to 3%) of graphite. The graphite chips had been heated (1050 °C) and degassed in vacuum (10^{-5} mbar) for one day and then stored in a dried argon atmosphere. The sample pellets were annealed at 650 °C for 3 days and cooled to room temperature at a rate of 10 °C/hr. All subsequent sample manipulations, including preparations for pressure experiments, were done in dry argon atmosphere.

The phase composition was checked by laboratory-based powder x-ray diffraction measurements using $\text{Cu K}\alpha_1$ radiation; these showed La_2C_3 as the majority phase ($\sim 85\%$) with a lattice parameter of 8.8150(6) Å. Weak additional reflections were observed which are attributed to an impurity phase of tetragonal LaC_2 ($a=3.9323(6)$ Å, $c=6.574(1)$ Å), its overall fraction being less than $\sim 15\%$. The superconducting properties of the sample were determined by resistivity, magnetic susceptibility, and heat capacity measurements. The resistive transition (midpoint) and the onset of diamagnetic shielding occurs at $T_c^{\text{onset}}=13.5(1)$ K (see Fig. 2). The width of the resistive transition (10%-90% criterion) amounts to 0.1 K. The heat capacity proves bulk superconductivity with a characteristic anomaly at T_c of $\Delta C_p/(\gamma T_c) \approx 2.2$; the deviation from the standard BCS anomaly is most likely due to enhanced electron-phonon coupling.

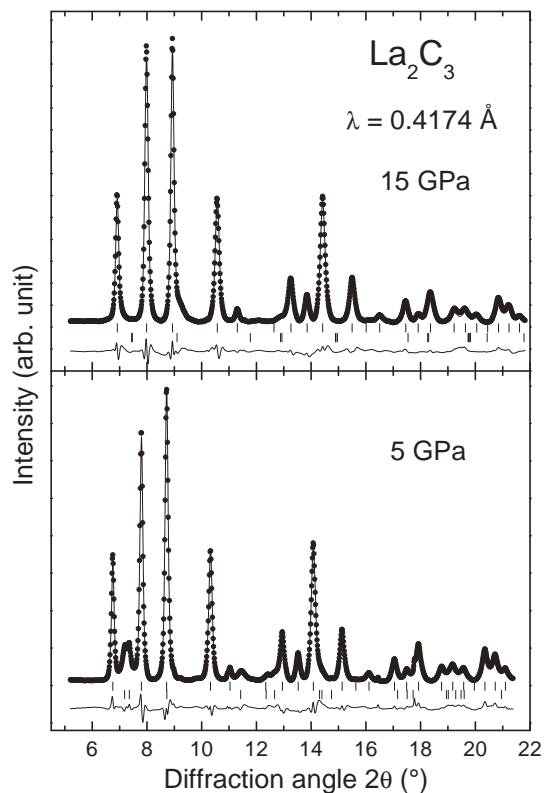


FIG. 3: Observed, calculated, and difference x-ray powder diffraction patterns for La_2C_3 at 5.0 and 15 GPa. The diffraction patterns were refined assuming an admixture of a tetragonal LaC_2 phase.¹⁴ Vertical markers indicate Bragg reflections of the two phases.

For the synchrotron x-ray diffraction measurements the sample was ground to a fine powder and a small amount of the powder was transferred into the gasket of a diamond anvil cell. Nitrogen was used as a pressure medium. When nitrogen solidifies (2.5 GPa at 300 K), it causes some additional Bragg reflections (typically weak) due to its various high-pressure phases. Angle-dispersive powder x-ray diffraction patterns (wavelength $\lambda = 0.4176$ Å) were measured at the beamline ID9 of the European Synchrotron Radiation Facility, Grenoble, using image plate detection. The images were integrated using the program FIT2D to yield intensity versus 2θ diagrams.¹⁵ To improve powder averaging, the DAC was oscillated by $\pm 3^\circ$. The ruby luminescence method was used for pressure measurement.^{16,17}

III. RESULTS AND DISCUSSION

Figure 3 shows representative diffraction diagrams of La_2C_3 collected at 5 and 15 GPa. The cubic phase of La_2C_3 was observed up to the highest pressure of this study, 30.7 GPa, and after releasing pressure. Extra Bragg reflections seen in the diffraction diagrams are consistent with the presence of tetragonal LaC_2 (SG

$I4/mmm$, No. 139, $Z=4$)e. The reflections due to LaC_2 gradually disappeared in the pressure range 10-13 GPa. Upon releasing pressure, the tetragonal phase was clearly present again at ambient conditions.

The diffraction patterns were analyzed by the Rietveld method using the program GSAS.^{18,19} The refined parameters of the sesquicarbide phase (space group $\bar{I}43d$) were the lattice constant, the fractional coordinate (x, x, x) of the 16c (La) site, a common isotropic thermal parameter for all atom sites, a Chebyshev polynomial background, Pseudo-Voigt profile function parameters, and an overall intensity scaling factor. The refinements were not sensitive to the exact value of the positional parameter v , 0, 0.25 of the carbon 24d site. Hence, v was fixed at 0.3049 (Ref. 3), corresponding to a C-C distance of 1.236 Å at ambient, and assumed independent of pressure. A preferred orientation correction was applied, but was found to result in only minor improvements of the refinements. Two-phase refinements were performed in order to account for the admixture of tetragonal LaC_2 , but only the unit cell parameters were refined for this phase; its internal parameter for the carbon position was assumed constant ($z=0.4024$,¹⁴ corresponding to a C-C distance of 1.284 Å at ambient). Figure 3 illustrates the results of the refinements for the two patterns collected at 5.0 and 15.0 GPa. The convergence was achieved at residuals (with a subtracted background) $R_{wp} = 8.7\%$ for 5 GPa and at $R_{wp} = 8.2\%$ for 15 GPa.

The experimental pressure-volume data of La_2C_3 are shown in Fig. 4. At 30 GPa, La_2C_3 is compressed by 18% and the volume is comparable to that of Y_2C_3 at ambient conditions. The pressure-volume data were fitted by a Birch equation of state²⁰

$$P(x) = \frac{3}{2}B_0 \cdot [x^{-7} - x^{-5}] \times \left[1 - \frac{3}{4}(B'_0 - 4)(1 - x^{-2}) \right], \quad (1)$$

where $x = (V/V_0)^{1/3}$ is a reduced length. The parameters are the volume V_0 , the bulk modulus B_0 , and its pressure derivative B'_0 , all at zero pressure. The fitted parameters and their standard deviations are given in Table I. The obtained value for V_0 is consistent with literature data.^{3,8}

Among the sesquicarbide compounds with the cubic Pu_2C_3 -type structure, La_2C_3 has the largest lattice parameter and therefore is expected to represent the most compressible candidate in this family of compounds.

TABLE I: Summary of fitted equation-of-state parameters (V_0 , B_0 , and B' , see Eq. 1) for cubic La_2C_3 and tetragonal LaC_2 . The V_0 values refer to the volume of the respective conventional unit cell. Also listed is V_0^{meas} which refers to the ambient-pressure value measured with $\text{Cu K}\alpha_1$ radiation.

Compound	V_0^{meas} (Å ³)	V_0 (Å ³)	B_0 (GPa)	B'
La_2C_3	684.96	686.6(4)	89.0(20)	5.5(3)
LaC_2	101.65	102.3(3)	76.3(90)	4.6(15)

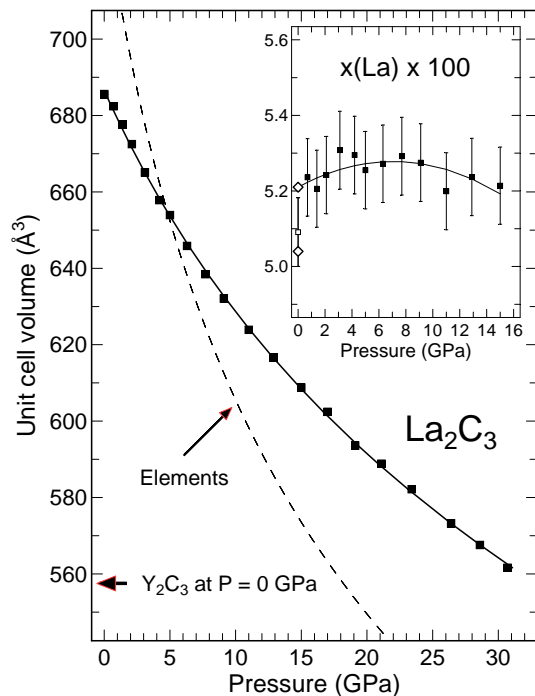


FIG. 4: Unit cell volume of La_2C_3 as a function of pressure. The solid line refers to a fitted Birch relation. The dashed line sketches the PV relation of the elemental constituents La metal and carbon (diamond form) taken in appropriate amounts. The inset shows the positional parameter $x(\text{La})$ as a function of pressure. Solid symbols are for data measured under pressure, open symbols are used to represent the x -value obtained after pressure cycling and corresponding literature data.^{3,8}

There appears to be no experimental data available on the bulk moduli of other cubic rare earth sesquicarbides to compare with. The bulk modulus of La_2C_3 at 30 GPa is about 250 GPa. This value would be an upper limit for the ambient-pressure bulk modulus B_0 of Y_2C_3 ; it is much lower than the calculated one ($B_0 = 363$ GPa) reported in Ref. 4.

At ambient conditions, the volume per La_2C_3 formula unit (85.68 Å³) is smaller than that of the constituents La metal and carbon in the diamond modification (La metal 37.5 Å³/La, diamond 5.67 Å³/C, $2 \times 37.5 + 3 \times 5.67 = 92.0$ Å³). So, the $P\Delta V$ term in the free energy difference favors the formation of the compound under pressure. However, because of the large compressibility of La metal [$B_0(\text{La}) \approx 25$ GPa, Ref. 21], the $P\Delta V$ term changes sign at about 5 GPa (Fig. 4). Hence, La_2C_3 is not necessarily a thermodynamically stable phase at all pressures covered in our experiment. A high-temperature experiment performed above 5 GPa may result in decomposition or, perhaps, the formation of a metal-rich carbide.

The Pu_2C_3 -type structure is closely related to the anti- Th_3P_4 -type. This similarity becomes obvious when writing the stoichiometry as $\text{La}_4(\text{C}_2)_3$ instead of La_2C_3 . The metal atoms in the Pu_2C_3 structure form a 3D network

of condensed RE_8 bisphenoids. The dicarbide anions are centered at the interstitial 12a site ($3/8, 0, 1/4$) and oriented along the $\bar{4}$ axes of the bisphenoids (Fig. 1) whose shape depends on the positional parameter x .^{22,23} For La_2C_3 we have $x(\text{La}) \approx 0.05$ which is intermediate between nearly equal lengths of all edges ($x \approx 1/32$) and equal center-corner distances ($x = 1/12$). Near $x = 0.05$ the metal-metal coordination is $3 + 2 + 6$ and the bisphenoids can host elongated entities.

Within the uncertainty of our data, the positional parameter $x(\text{La})$ stays constant under pressure (Fig. 4). This means that the coordination polyhedron around C_2 is compressed isotropically, and there is no change in the second neighbor coordination. Actually, at ambient pressure the x parameters of all cubic rare earth and actinide sesquicarbides cluster around 0.051 with a quite narrow spread of ± 0.002 .²⁴

The arrangement of metal ions in La_2C_3 is similar to that of the 'cI16' (16-atom body centered cubic) phase of high-pressure Li which can be interpreted as a $2 \times 2 \times 2$ superstructure of bcc.²⁵ In Li-cI16 a pseudo-gap is formed, involving a lowering of the density of states $N(E_F)$ at the Fermi level, which leads to a decrease of the total energy relative to any of the common high-symmetry phases of elemental metals. Despite the pseudo-gap formation, the cI16 phase of Li is a superconductor with $T_c > 10$ K (see Ref. 26 and literature cited therein). As for La_2C_3 , the Fermi level is calculated to also fall into a local minimum of the DOS.²⁷ This is qualitatively similar to what is reported for Y_2C_3 .^{4,5} It is not clear whether the formation of a local DOS minimum in the sesquicarbides is a consequence of the structural distortion of the metal sublattice away from bcc. In any case, the states in the DOS minimum of Y_2C_3 show a strong coupling to 'symmetry-preserving' metal atom displacements, i.e. a change in the x parameter.⁵

For La_2C_3 , a C-C distance of 1.236 \AA is given in Ref. 3. A slightly larger distance, about 1.29 \AA (Ref. 8), appears more plausible. Unfortunately, our experiments do not provide any information on the pressure dependence of the C-C distance. This distance will correlate

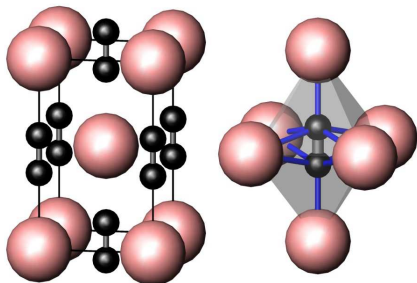


FIG. 5: (Color online) The tetragonal CaC_2 -type crystal structure of LaC_2 [SG $I4/mmm$ (No. 139), $Z = 2$, $a = 3.937$, $c = 6.580$, La in 2a (0,0,0), C in 4e (0,0, z), $z = 0.4026$, distance C-C = 1.289 \AA , after Ref. 14]. The C_2 units, oriented along c , are sixfold coordinated by La.

with the degree of charge transfer between La d and antibonding (π^*) states of the C_2 unit. We can expect that the back-donation effect increases with pressure.

We now turn to LaC_2 , the impurity phase in our sample. LaC_2 crystallizes in a body-centered tetragonal structure (Fig. 5). The C_2 units in LaC_2 (C-C distance 1.28 \AA) are reported to be oriented parallel to the c axis^{14,28}; they are sixfold coordinated by La atoms which form elongated octahedra.

The pressure-volume data of LaC_2 are shown in Fig. 6. Parameters obtained by fitting a Birch relation to the high-pressure data are given in Table I. The back-extrapolated zero pressure volume given in Table I is 0.3% larger than $V_0 = 102.0 \text{ \AA}^3$ measured after pressure cycling. The latter value agrees with Ref. 14. Despite the larger carbon to metal ratio, the bulk modulus of LaC_2 comes out slightly lower compared to La_2C_3 . This may be explained by the larger metal-metal distance in LaC_2 ($12 \times 3.93 \text{ \AA}$ at ambient pressure) compared to the average value for La_2C_3 ($3 \times 3.63 \text{ \AA}$, $2 \times 3.81 \text{ \AA}$, $6 \times 4.01 \text{ \AA}$). The inset of Fig. 6 illustrates that the c/a ratio of LaC_2 increases with increasing pressure, i.e., the compressibility is smaller along the direction of the dumbbell orientation.

The diffraction pattern of LaC_2 was completely lost at pressures above 13 GPa, but it reappeared upon releasing pressure. It is left to a separate study to find out whether LaC_2 undergoes a reversible pressure-induced phase transition. Already at ambient pressure, the volume of LaC_2 is larger than that of the constituents ($\text{LaC}_2 = 51 \text{ \AA}^3$ per formula unit at $P=0$, $\text{La} + 2 \text{ C} = 48.84 \text{ \AA}^3$). So, application of pressure should be a strong driving force for a phase change, not ruling out at this point a pressure-induced amorphization as a precursor to phase separation. Another question, brought up by studies of CaC_2

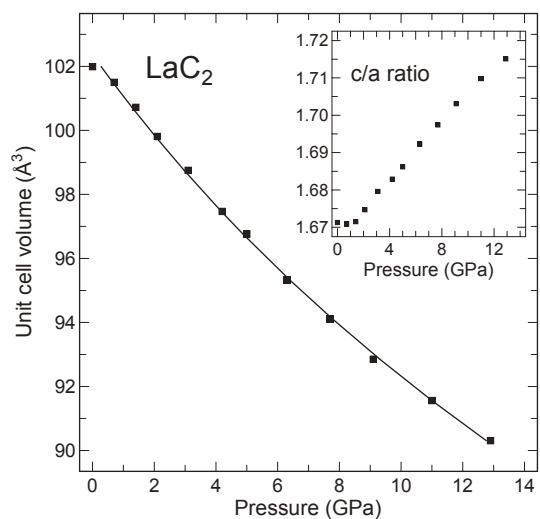


FIG. 6: Unit cell volume of tetragonal LaC_2 as a function of pressure. The solid line refers to a fitted Birch relation. The inset shows the c/a ratio as a function of pressure.

at ambient pressure,^{29,30} concerns the orientation of the C₂ dumbbells in tetragonal LaC₂. Our data point to a possible *c/a* anomaly near ambient pressure (see inset of Fig. 6) which could be related to a pressure-dependent reorientation.

In conclusion, the present high-pressure structural study gives quantitative information on the equation

of state and structural parameters of superconducting La₂C₃. The results may serve as a reference for the as yet unknown high-pressure behavior of other cubic rare earth sesquicarbides. The results are also believed to provide useful input for modelling the pressure-dependence of the electronic structure and the electron-phonon coupling of La₂C₃.

-
- * Corresponding author: E-mail k.syassen@fkf.mpg.de
- ¹ G. Amano, S. Akutagawa, T. Muranaka, Y. Zenitani, and J. Akimitsu, *J. Phys. Soc. Jpn* **73**, 530 (2004).
 - ² T. Nakane, T. Mochiku, H. Kito, J. Itoh, M. Nagao, H. Kamakura, and Y. Takano, *Appl. Phys. Lett.* **84**, 2859 (2004).
 - ³ M. Atoji and D. Williams, *J. Chem. Phys.* **35**, 1960 (1961).
 - ⁴ I. R. Shein and A. L. Ivanovskii, *Solid State Commun.* **131**, 223 (2004).
 - ⁵ D. J. Singh and I. I. Mazin, *Phys. Rev. B* **70**, 052504 (2004).
 - ⁶ F. H. Spedding, K. A. Gschneidner jr., and A. H. Daane, *Trans. AIME* **215**, 192 (1959).
 - ⁷ K. A. Gschneidner and F. W. Calderwood, *Bull. Alloy Phase Diagr.* **7**, 86 (1986). **7**, 86 (1986).
 - ⁸ A. Simon and T. Gulden, *Z. Anorg. Allg. Chem.* **630**, 2191 (2004).
 - ⁹ T. Gulden, Ph.D. thesis, Universität Stuttgart (1997).
 - ¹⁰ A. L. Giorgi, E. G. Sklarz, M. C. Krupka, and N. H. Krikorian, *J. Less-Common Met.* **17**, 121 (1969).
 - ¹¹ A. L. Giorgi, E. G. Sklarz, N. H. Krikorian, and M. C. Krupka, *J. Less-Common Metals* **22**, 131 (1970).
 - ¹² T. L. Francavilla and F. L. Carter, *Phys. Rev. B* **14**, 128 (1976).
 - ¹³ R. W. Henn, Ph.D. thesis, Universität Karlsruhe (1996).
 - ¹⁴ D. W. Jones, I. J. McColm, and J. Yerkees, *J. Solid State Chem.* **92**, 301 (1991).
 - ¹⁵ A. P. Hammersley, S. O. Svensson, M. Hanfland, A. N. Fitch, and D. Häussermann, *High Pressure Research* **14**, 235 (1996).
 - ¹⁶ G. J. Piermarini, S. Block, J. D. Barnett, and R. A. Forman, *J. Appl. Phys.* **46**, 2774 (1975).
 - ¹⁷ H. K. Mao, J. Xu, and P. M. Bell, *J. Geophys. Res.* **91**, 4673 (1986).
 - ¹⁸ A. C. Larson and R. B. van Dreele, *GSAS: General Structure Analysis System*, Los Alamos National Laboratory Report LAUR 86-748 (2000).
 - ¹⁹ B. H. Toby, *J. Appl. Cryst.* **34**, 210 (2001).
 - ²⁰ F. Birch, *J. Geophys. Res.* **83**, 1257 (1978).
 - ²¹ K. Syassen and W. Holzapfel, *Solid State Commun.* **16**, 533 (1975).
 - ²² B. G. Hyde and S. Andersson, *Inorganic Crystal Structures* (Wiley, New York, 1989).
 - ²³ W. Carillo-Cabrera, J. Curda, K. Peters, and H. G. von Schnering, *J. Solid State Chem.* **147**, 372 (1999).
 - ²⁴ ICSD, *Inorganic Crystal Structure Database*, Fachinformationszentrum (FIZ) Karlsruhe, Release 2003.
 - ²⁵ M. Hanfland, K. Syassen, N. E. Christensen, and D. Novikov, *Nature* **408**, 174 (2000).
 - ²⁶ S. Deemyad and J. S. Schilling, *Phys. Rev. Lett.* **91**, 167001 (2003).
 - ²⁷ J. S. Kim, R. K. Kremer, O. Jepsen, and A. Simon, *Curr. Appl. Phys.* **xx**, xx (2005), submitted.
 - ²⁸ A. L. Bowman, N. H. Krikorian, G. Arnold, T. Wallace, and N. G. Nereson, *Acta Cryst. B* **24**, 459 (1968).
 - ²⁹ J. R. Long, R. Hoffmann, and H. J. Meyer, *Inorganic Chemistry* **31**, 1734 (1992).
 - ³⁰ M. Knapp and U. Ruschewitz, *Chem. Eur. J.* **7**, 874 (2001).